Excitonic fractional quantum Hall hierarchy in moiré heterostructures

Yves H. Kwan, Yichen Hu, Steven H. Simon, and S. A. Parameswaran
Rudolf Peierls Centre for Theoretical Physics, Clarendon Laboratory, Oxford OX1 3PU, United Kingdom

(Received 15 April 2020; revised 26 March 2022; accepted 3 June 2022; published 16 June 2022)

We consider fractional quantum Hall states in systems where two flat Chern number $C = \pm 1$ bands are labeled by an approximately conserved valley index and interchanged by time reversal symmetry. At filling factor $\nu = 1$ this setting admits an unusual hierarchy of correlated phases of *excitons*, neutral particle-hole pair excitations of a fully valley-polarized orbital ferromagnet parent state where all electrons occupy a single valley. Excitons experience an effective magnetic field due to the Chern numbers of the underlying bands. This obstructs their condensation in favor of a variety of crystalline orders and gapped and gapless liquid states. All these have the *same* quantized charge Hall response and are electrically incompressible, but differ in their edge structure, orbital magnetization, and hence valley and thermal responses. We explore the relevance of this scenario for moiré heterostructures of bilayer graphene on a hexagonal boron nitride substrate.

DOI: 10.1103/PhysRevB.105.235121

The observation of gate-tunable superconductivity and correlated insulating behavior in twisted bilayer graphene (TBG) in the magic angle regime [1,2] has stimulated intense investigation of two-dimensional (2D) van der Waals heterostructures. While the precise mechanism behind the high superconducting transition temperatures (relative to the low carrier density) remains hotly debated, intrinsic to this setting is the enhancement of correlations when the electronic dispersion is reconstructed by the interlayer moiré pattern corresponding to a small twist angle. After accounting for spin and valley degeneracies, substrate-free TBG hosts eight flattened central bands that are interlinked by Dirac points and energetically separated from remote bands. This quenching of the single-particle kinetic energy bears a family resemblance to the formation of Landau levels (LLs) by 2D electron gases in magnetic fields. The analogy is sharpened if one or more of the graphene layers are aligned with the encapsulating hexagonal boron nitride (hBN) substrate: this opens topological gaps at the Dirac points, pushing four bands above (below) the neutrality point while assigning each band a nonzero Chern number ($C = \pm 1$) in a manner that preserves overall time-reversal symmetry (TRS) [3–5].

Flat Chern bands with $|C| = 1$ are similar to LLs: when fully filled, they show a quantized anomalous Hall (QAH) response [6–8], the lattice analog of the integer quantum Hall (QH) effect [9]. At commensurate partial fillings, interactions can stabilize incompressible fractional Chern insulators (CIs) [10,11]. However, most realizations of CIs, e.g., in magnetic topological insulators [12] or cold atomic gases [13] have significant single-particle dispersion and hence relatively weak correlations.

The observation of a QAH response in hBN-TBG devices at filling $\nu = +3$ relative to charge neutrality in the absence of an external magnetic field [14] points to the breaking of TRS by interactions [3,5,15–18], leading to selection of a spin- and valley-polarized insulating state corresponding to fully filling a single Chern band. While reminiscent of quantum Hall ferromagnetism (QHFM) in LLs, an important distinction in hBN-TBG is that TRS is broken *spontaneously*, lifting the degeneracy between two valleys with equal and opposite Chern number. These systems are robust and tunable platforms to study correlated Chern insulators and proximate phases [19–21].

Here, we propose that systems such as hBN-TBG and related heterostructures [22], where two nearly-flat degenerate Chern bands have equal and opposite Chern number, are unique settings for an unconventional *excitonic quantum Hall hierarchy*. The excitons we consider are stable neutral gapped intervalley excitations of the fully-valley-polarized insulator, that are bound states of a hole in a filled Chern band and a particle in an empty band with the opposite Chern number. Tightly bound excitons can be viewed — in a sense we make precise in a companion paper [23] — as neutral bosons in a Chern band. As in TBG we take the bands to correspond to different valleys; assuming valley conservation we may then meaningfully view the excitons as filling a Chern band. The exciton filling tracks the change in valley polarization relative to the fully polarized parent state. We show using a simplified LL model [3] that the fully valley polarized phase is proximate to a rich hierarchy of correlated phases that emerge when interactions between excitons lead them to form incompressible bosonic fractional quantum Hall (FQH) liquid states, a variety of Wigner crystal or stripe/bubble phases with broken translational symmetry, or compressible Fermi-liquid-like states (CFLs). All the incompressible states (and some of the compressible ones) have identical charge response, namely a quantized Hall conductivity $\sigma_{xy} = e^2/h$ and vanishing longitudinal conductivity $\sigma_{xx} = 0$, but differ in their valley and thermal Hall responses. We suggest experimental probes to distinguish the various excitonic phases. Finally, we discuss how the delicate balance of energy scales from interactions, gate screening, and the residual band dispersion

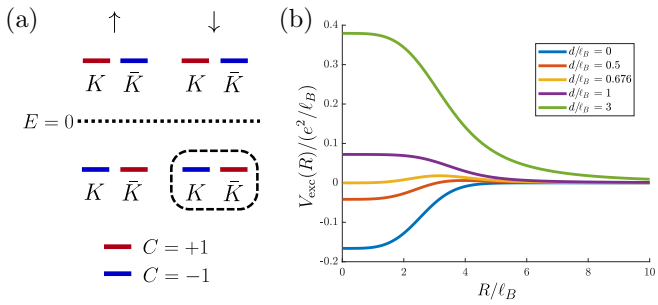

FIG. 1. (a) Schematic of eight central bands and Chern numbers in hBN-TBG; our model focuses on a pair of these (dashed box). (b) Exciton-exciton interaction profile as competition of inter/intravalley interactions is tuned by d.

could stabilize this excitonic FQH hierarchy within the phase diagram of hBN-TBG or other moiré systems.

I. MODEL AND FULLY VALLEY-POLARIZED PARENT STATE

We are ultimately interested in the eight central bands of TBG at fillings $\nu = \pm 3, \pm 1$. Here, $\nu = 0$ corresponds to charge neutrality, and $\nu = -4(+4)$ corresponds to the case where all these eight bands are empty (filled) [Fig. 1(a)]. The hBN substrate opens a single-particle gap at neutrality resulting in bands with Chern numbers $C^{>}_{K,\sigma} = -C^{<}_{K,\sigma} = -C^{>}_{\bar{K},\sigma} = C^{<}_{\bar{K},\sigma} = 1$ where $>$ ($<$) labels bands above (below) neutrality and we have introduced valley $\tau = K, \bar{K}$ and spin $\sigma = \uparrow, \downarrow$ labels [3,5,15]. Throughout, we ignore spin-orbit coupling and elevate approximate valley conservation to an exact $U(1)_v$ symmetry. The noninteracting band structure thus has $SU(2)_s \times U(1)_v \times U(1)_c$ symmetry (where c, v, s refer to charge, valley, and spin), and preserves TRS which interchanges the valleys and flips the sign of C.

In order to study interaction effects at odd integer filling we introduce several simplifications. First, we work with a model interaction projected to the relevant bands and ignore mixing between bands split at the single-particle level. Second, we suppress the spin degree of freedom and restrict our attention to the partially filled doublet of degenerate valleys $K, \bar{K}$ with equal and opposite Chern numbers [Fig. 1(a)]. Finally, in line with previous studies [3] we replace the Chern bands with LLs where valleys $K, \bar{K}$ see equal and opposite magnetic fields. We note that these are reasonable approximations appropriate to the flat-band limit of interest that nevertheless capture the underlying topological band structure. The single-particle Hamiltonian in valley $\tau = \pm$ (henceforth we use valley index and Chern number interchangeably as they are tied together in the two-valley subspace) takes the form $H_{\pm} = \frac{(\boldsymbol{p} \mp e\boldsymbol{A})^2}{2m}$ with $\boldsymbol{\nabla} \times \boldsymbol{A} = B$. We assume each valley is in its N_Φ-fold degenerate lowest LL; here $N_\Phi = A/2\pi\ell_B^2$ counts the number of flux quanta threading sample area A, and $\ell_B = (\hbar/eB)^{1/2}$ is the magnetic length (which plays the role of the moiré scale in TBG). We fix the filling factor of this pair of LLs at $\nu = \nu_+ + \nu_- = 1$, where $\nu_\pm = N_\pm/N_\Phi$ is the filling factor in each valley. The effective Hamiltonian consists of interactions projected onto the degenerate LLs,

$$H_{\text{int}} = \frac{1}{2N_\Phi} \sum_{\mathbf{q},\tau,\tau'} V_{\tau\tau'}(\mathbf{q}) : \bar{\rho}_\tau(\mathbf{q}) \bar{\rho}_{\tau'}(-\mathbf{q}) : . \tag{1}$$

Here, we have introduced the projected density operators

$$\bar{\rho}_\pm(\mathbf{q}) = F(\mathbf{q}) \sum_{k_y} e^{\pm i q_x k_y \ell_B^2} c^\dagger_{k_y - \frac{q_y}{2},\pm} c_{k_y + \frac{q_y}{2},\pm}, \tag{2}$$

where $F(\mathbf{q}) = e^{-\mathbf{q}^2\ell_B^2/4}$ and $c^\dagger_{k_y,\pm}$ is the creation operator of a Landau-gauge single-particle lowest-LL state $\phi_{k_y,\pm}(x) = \frac{e^{ik_y y} e^{-(x \mp k_y \ell_B^2)^2/2\ell_B^2}}{\sqrt{L_y \ell_B \sqrt{\pi}}}$. We choose a phenomenological interaction that only includes density-density terms, $V_{\tau,\tau}(\mathbf{q}) = v(\mathbf{q}) = \frac{2\pi e^2}{|\mathbf{q}|}$, $V_{\tau,-\tau}(\mathbf{q}) = v_d(\mathbf{q}) = v(\mathbf{q}) e^{-|\mathbf{q}|d}$, where d tunes the competition of inter- and intravalley interactions. Other intervalley terms are $o(a_0/\ell_B)$ where a_0 is a lattice scale tied to the separation of valleys in the microscopic BZ.

Equation (1) is essentially the LL limit of a minimal model for TBG introduced in Ref. [3], absent a periodic potential and with slightly modified interactions. There, within a Hartree-Fock (HF) analysis it was argued that the ground state of (1) is a fully-valley-polarized insulator (FVPI) that with $\nu_+ = 1, \nu_- = 0$. This state has a QAH response linked to the spontaneous breaking of TRS. The FVPI was argued to be stable against both the inclusion of a weak nonzero single-particle dispersion, as well as allowing $d > 0$. Although the former is also true for conventional QHFMs where all bands have $C = 1$, the latter is unexpected: arguing in analogy with bilayer QH systems, we would anticipate that softening the intervalley interactions in this way would stabilize intervalley-coherent states with $\nu_+ = \nu_- = \frac{1}{2}$. However when $C_+ = -C_-$, even for $d \to 0$ the symmetry is reduced relative to the $C_+ = C_-$ [3] case. This is evident, e.g., in the gap to "valley-flip" excitations of the FVPI, that persists in more microscopic models of TBG [23,24].

II. EXCITON TOPOLOGY AND INTERACTIONS

A more striking consequence of the reversal of Chern numbers between the valleys lies in the topological structure of intervalley excitations. Consider a single inter-valley particle-hole pair excitation of the FVPI. Up to an overall constant loss of exchange energy in creating a single hole, in the LL limit the Hamiltonian is that of an electron and a hole in equal and opposite magnetic fields $\mp B$, with *attractive* intervalley interactions, $H_{\text{ex}} = \frac{(\boldsymbol{p}_e + e\boldsymbol{A})^2}{2m} + \frac{(\boldsymbol{p}_h + e\boldsymbol{A})^2}{2m} - v_d(\mathbf{r})$, where $v_d(r) = \int \frac{d\mathbf{q}}{(2\pi^2)} e^{-i\mathbf{q}\cdot\mathbf{r}} v_d(\mathbf{q})$. The applicability of this effective Hamiltonian to the physics in the single particle-hole subspace is numerically verified in Ref. [23]. This decouples in terms of relative $\mathbf{r} = \mathbf{r}_h - \mathbf{r}_e$ and center-of-mass $\mathbf{R} = \frac{\mathbf{r}_h + \mathbf{r}_e}{2}$ coordinates, yielding $H_{\text{ex}} = H_{\mathbf{R}} + H_{\mathbf{r}}$, with

$$H_{\mathbf{R}} = \frac{(\boldsymbol{P}_{\text{CM}} + 2e\boldsymbol{A})^2}{4m}, H_{\mathbf{r}} = \frac{\left(\boldsymbol{p}_{\text{rel}} + \frac{e}{2}\boldsymbol{A}\right)^2}{m} - v_d(r). \tag{3}$$

Accordingly, each discrete excitonic bound-state solution of $H_{\mathbf{r}}$ has a $2N_\Phi$-fold degeneracy corresponding to the LL degeneracy of $H_{\mathbf{R}}$. Explicitly, if z_e, z_h are complex coordinates for the electron and hole respectively, defining $z = \frac{z^e + z^h}{2}$ and

$u = z^h - z^e$ and freezing the relative coordinate u in the lowest excitonic bound state ϕ_0 yields

$$\psi_{\rm exc}(z,u) = \tilde{f}(z)e^{-|z|^2/2}\phi_0(u) \text{ with } \phi_0(u) \equiv e^{-|u|^2/8}, \quad (4)$$

where $\tilde{f}$ is analytic and we take $\ell_B = 1$ [25]. Note that z (u) sees an effectively doubled (halved) field, consistent with (3). Exciton structure is more complicated in realistic models that include the dispersion and Berry curvature fluctuations of the underlying bands, and both the form of the envelope function ϕ_0 and its coupling to center-of-mass motion can influence exciton topology. Nevertheless, the lowest exciton band has $C \neq 0$ for a range of parameters even in realistic models of hBN-TBG [23]. Even beyond this regime, exciton bands have substantial Berry curvature, which can influence phase structure even if the Chern number (its integral over the BZ of allowed exciton momenta [23]) vanishes.

Each exciton also carries a unit of $U(1)_v$ valley polarization. Since the latter is conserved it is meaningful to consider partial valley-polarized states corresponding to a finite density of excitons. For instance, intervalley-coherent exciton condensate HF trial states with $\nu_+ = \nu_- = \frac{1}{2}$ are energetically uncompetitive in much of the phase diagram because exciton topology forces them to host a vortex lattice analogous to Type-II superconductors in a magnetic field [3]. Evidently, as bosons in a magnetic field the excitons can form various other many-body states inaccessible to a HF analysis, depending on the effective exciton-exciton interaction $V_{\rm exc}(R)$. For our choice of $v(\mathbf{r})$ we estimate $V_{\rm exc}(R)$ by considering appropriately antisymmetrized variational wave functions for a pair of tightly bound excitons at separation R [25]; representative results are sketched in Fig. 1(b). Short-range interactions are repulsive (attractive) if $d/\ell_B \gtrsim 1$ ($\lesssim$). For any $d > 0$ excitons experience an asymptotic R^{-3} repulsion that vanishes for $d = 0$. (A power-law tail is generically expected, but its exponent may depend on the choice of $v(\mathbf{r})$.) A second subtlety in considering many-body exciton phases is that single-exciton states are not all independent [26].

While this is unimportant in the dilute limit $\nu_- = 1 - \nu_+ \ll 1$, we will be interested in fillings $\nu_- = 1/m$ where m is not necessarily large. Below we will ignore this subtlety and consider the excitons as *bona fide* bosons.

III. EXCITON FQH HIERARCHY

With these preliminaries, we now turn to possible excitonic phases. We consider fillings $(\nu_+, \nu_-) = (1 - \nu_v, \nu_v)$ with $0 < \nu_v < \frac{1}{2}$, corresponding to adding $\nu_v N_\Phi$ intervalley excitons to the FVPI resulting in valley polarization $I^z_v = \frac{1}{2} - \nu_v$ per electron. Since all terms have characteristic scale $\sim e^2/\ell_B$ the phase structure hinges on microscopic details of the interactions. For now we assume that exciton binding sets the dominant scale and that the interexciton interaction $V_{\rm exc}$ is always repulsive and short ranged. (We comment on other cases below.) In this regime, it is reasonable to assume that the exciton is a stable bound state. Since each exciton behaves as though it occupies a $2N_\Phi$-fold degenerate LL, the effective filling factor is $\nu_b = \nu_v/2$. For $\nu_v = 1/m$ with m an integer, the tightly bound excitons can form a $\nu_b = 1/2m$ bosonic Laughlin state. A trial wave function that captures this is given by

$$\begin{aligned}\Psi_{2m}(\{z^e, z^h\}) &= \mathcal{P}_{\rm exc}[\Psi_m(\{z^e\})\Psi_m(\{z^h\})] \\ &= \sum_{\sigma \in S_N} \operatorname{sgn}\sigma \left[\Psi_m(\{z_{i,\sigma(i)}\})^2 \prod_j \phi_0(u_{j\sigma(j)})\right].\end{aligned} \quad (5)$$

Here, $\Psi_m(\{z\}) = \prod_{i<j}(z_i - z_j)^m e^{-\sum_i \frac{|z_i|^2}{4}}$ and $\mathcal{P}_{\rm exc}$ projects electron-hole pairs into the excitonic ground state ϕ_0 (4). This antisymmetrizes over permutations $\sigma \in S_N$ corresponding to different pairings of the $N = N_\Phi/m$ electrons i and holes $\sigma(i)$ to form excitons centered at $z_{i\sigma(i)} = \frac{1}{2}(z^e_i + z^h_{\sigma(i)})$ at separation $u_{i\sigma(i)} = z^h_i - z^e_{\sigma(i)}$ and then projects the latter into ϕ_0 [25]. $\Psi_{2m}(\{z^e, z^h\})$ is a many-particle state of electrons in valley '−' and holes in valley '+', built on top of the FVPI parent state vacuum. Particle-hole (PH) transforming Eq. (5) only in the '+' valley yields a purely electronic wave function.

An alternative picture of the excitonic phase structure is obtained by viewing the problem (after PH transformation to holes in valley '+') as a two-valley system where each component sees the *same* magnetic field and is at filling $\nu = 1/m$, and where inter (intra) valley interactions are attractive (repulsive) [27]. This gives distinct pictures for odd and even m. (In each case, the electronic state is obtained after undoing the PH transformation.)

For even m, we can attach m quanta of flux to each valley separately, yielding an equal density of composite fermions (CFs) in each valley. For weak intervalley attraction we anticipate that these are stable against pairing [28], yielding a compressible state. For increasing attraction, we expect a transition into an intervalley paired state of CFs, schematically given by

$$\Psi^{\rm CF}_{2m} \sim \mathcal{P}_L \prod_{i<j} \left(z^e_i - z^e_j\right)^m \prod_{k<l} \left(z^h_k - z^h_l\right)^m \det\left[g\left(z^e_i - z^h_j\right)\right], \quad (6)$$

where the determinant describes pairing with wave function $g(z)$, $\mathcal{P}_L$ projects to the lowest LL and we have omitted Gaussian factors. For s-wave or strong-coupling higher-angular momentum pairing we expect $g(z) \sim e^{-z/\xi}$ as $z \to \infty$, where $\xi \sim o(\ell_B)$ is the pair size. Qualitatively, this pairs electrons and holes into tightly bound bosons that then form a $\nu_b = 1/2m$ Laughlin state. This is consistent with our picture of Eq. (5), so we conclude that the two approaches describe similar physics. In non-s-wave cases, strong- and weak-pairing regimes are separated by a phase transition. For $p_x + ip_y$-pairing where $g(z) \sim 1/z$, this would be a transition between state (5) and the $(m-1, m-1, 1)$ Halperin state which also has $\nu = 1/m$ in each valley. [The equivalence of Eq. (6) with $p_x + ip_y$ pairing to the Halperin state follows via the Cauchy identity [29,30].] For $m = 4$, preliminary exact diagonalization studies [25] find a unique ground state in this valley polarization sector for $N = 4, 6, 8, 10$ particles on the sphere [31] at a shift [32] appropriate to Eq. (5) for certain short-range interactions. This suggests that the excitonic Laughlin state is energetically competitive as there is no other obvious incompressible candidate at this shift. (Note that this is not necessarily the global ground state across all valley sectors.)

For m odd and zero intervalley interactions each component forms an *independent* $\nu = 1/m$ fermionic Laughlin state. Intervalley attraction locks these together, suppressing fluctuations where a particle in one valley is far from a hole in the other. However, as each valley is independently incompressible, numerical observation of a unique ground state is less strong evidence for Eq. (5).

Other unconventional phases are also possible. For example, if $\nu_v = 2/q$ with q odd, the exciton filling is $\nu_b = 1/q$ ruling out bosonic Laughlin states. In this limit, attaching q quanta of $U(1)_v$ valley flux to each exciton gives rise to a compressible excitonic composite Fermi liquid (e-CFL). This does not obviously decouple into separate flux attachments to constituent electrons/holes. The e-CFL has intervalley binding but no valley coherence, and is hence distinct from interlayer coherent CFLs [33] proposed in QH bilayers. A more exotic possibility is that the e-CFL in turn can undergo p-wave pairing to form a non-Abelian QH state. The states considered here are specific examples of a rich hierarchy of FQH states of excitons, whose detailed analysis we defer to future work.

IV. EDGE STRUCTURE AND RESPONSE

We now discuss transport properties and bulk response of the states considered above. Since the excitonic Laughlin state (5) is a bosonic FQH state, we expect a quantized response in the charge carried by this state, which (translating back into the underlying electrons) leads to a fractional quantized valley Hall (QVH) response, $\sigma^v_{xx} = 0, \sigma^v_{xy} = -\nu_b \frac{q_v^2}{h} = -\frac{1}{2m}\frac{q_v^2}{h}$, where $q_v = 1$ is the valley charge of a single exciton. We can understand this also from an edge-state perspective. Before implementing exciton projection, in terms of the underlying electrons we can view the edge of Eq. (5) as built out of (i) a chiral $\nu_+ = 1$ chiral mode of electrons in a filled LL; (ii) a $\nu_+ = 1/m$ chiral edge mode of holes in valley '+'; and (iii) a chiral $\nu_- = 1/m$ edge of electrons in valley '−'. Owing to the opposite charge of holes and the opposite sign of B in the two valleys (ii) and (iii) counter-propagate relative to (i) and copropagate relative to each other. The exciton projection can then be viewed as binding the two copropagating fermionic FQH edge modes due to the attractive electron-hole interactions, leading to a single bosonic $\nu_b = 1/2m$ mode propagating upstream of the charge mode.

Other cases are more complicated. For $\nu_v = 1/m$ with m even and weak intervalley interactions, we find decoupled CFL-like states [27] in which the charge QH response breaks down in favor of metallic transport. In contrast, for $\nu_v = 2/q$ with q odd, since the exciton binding dominates, both compressible and incompressible phases have a charge QH response. In the compressible e-CFL state this coexists with metallic valley response from the exciton Fermi surface whereas the incompressible paired descendants of the e-CFL have a QVH response.

Experimentally, it is challenging to distinguish different exciton phases via electrical measurements, since nearly all of them have identical $\sigma_{xy} = e^2/h$ charge QH response. While it is difficult to directly measure the QVH response, upstream modes can be detected by measuring thermal conductance K_H [34]. If the upstream and downstream modes are fully thermally equilibrated, $K_H = 0$, whereas if they are out of equilibrium we expect a *doubled* response relative to the integer QH case. Phases with QVH response show plateaus in valley polarization quantized at a rational fraction of its value in the FVP that if measured, would be another diagnostic.

Crystalline Phases. So far we have ignored the long-range tail of $V_{\text{exc}}(R)$. While this is unlikely to destabilize FQH liquids favored by short-range repulsive interactions, the competition between short-range attraction and long-range repulsion [35] can drive the formation of vortex lattices and bubble and stripe phases [36,37]. Similarly at lower density, Wigner-crystal like phases of excitons can be formed [38]. These states, whose study we defer to the future, all have broken translational symmetry, and (if pinned by the moiré potential or disorder) can also show a charge QH response.

V. DISCUSSION

We have proposed a class of FQH state formed by the binding of electron-hole pairs in bands with equal and opposite Chern number. In closing, we return to our original goal of linking this to the physics of TBG, which has several key ingredients — flipped Chern numbers, flat bands, and interactions — that were pertinent to our analysis. However, our model leaves out other features such as band dispersion and Berry curvature fluctuations. Another concern is that numerics indicate that incompressible excitonic states are more stable if intravalley interactions are larger than intervalley couplings, whereas the leading long-range density-density interactions in TBG have the same magnitude independent of valley. Since the valley dependence of the short-range component of interactions is difficult to precisely determine, it is reasonable to explore a wider parameter regime allowing for asymmetry of intra- and intervalley couplings. HF studies [3] in a similar regime indicate that this competition can combine with nonzero dispersion to stabilize partially valley-polarized metals against the FVPI. It seems possible that the *incompressible* partially valley polarized excitonic FQH insulator studied here may be energetically competitive to these. Tuning valley occupation and band structure via perpendicular or parallel magnetic fields [3,39] could also stabilize excitonic phases. Another notable omission is electron spin, whose influence on interexciton interactions may further enrich the phase diagram. Looking beyond TBG, capacitive charging effects in multilayer moiré heterostructures may favor excitonic states, and intertwine valley and layer degrees of freedom so as to make the QVH response accessible. In the future, it will be interesting to apply similar ideas to other moiré and flat-band systems or strained graphene [40] and clarify their connection to fractional excitonic insulators proposed to form near topological band inversions far from the flat band limit [41].

Note added. After a preprint of this manuscript was made available on the arXiv, another work [42] has appeared that studies similar questions. Our results are in agreement where they overlap.

ACKNOWLEDGMENTS

We thank N. Bultinck, B. Lian, N. Regnault, S.L. Sondhi, and M.P. Zaletel for useful discussions. We acknowledge

support from the European Research Council (ERC) under the European Union Horizon 2020 Research and Innovation Programme (Grant Agreement No. 804213-TMCS) and from EPSRC grant EP/S020527/1.

[1] Y. Cao, V. Fatemi, A. Demir, S. Fang, S. L. Tomarken, J. Y. Luo, J. D. Sanchez-Yamagishi, K. Watanabe, T. Taniguchi, E. Kaxiras *et al.*, Correlated insulator behaviour at half-filling in magic-angle graphene superlattices, Nature (London) **556**, 80 (2018).

[2] Y. Cao, V. Fatemi, S. Fang, K. Watanabe, T. Taniguchi, E. Kaxiras, and P. Jarillo-Herrero, Unconventional superconductivity in magic-angle graphene superlattices, Nature (London) **556**, 43 (2018).

[3] N. Bultinck, S. Chatterjee, and M. P. Zaletel, Mechanism for Anomalous Hall Ferromagnetism in Twisted Bilayer Graphene, Phys. Rev. Lett. **124**, 166601 (2020).

[4] Y.-H. Zhang, D. Mao, Y. Cao, P. Jarillo-Herrero, and T. Senthil, Nearly flat chern bands in moiré superlattices, Phys. Rev. B **99**, 075127 (2019).

[5] Y.-H. Zhang, D. Mao, and T. Senthil, Twisted bilayer graphene aligned with hexagonal boron nitride: Anomalous hall effect and a lattice model, Phys. Rev. Research **1**, 033126 (2019).

[6] D. J. Thouless, M. Kohmoto, M. P. Nightingale, and M. den Nijs, Quantized Hall Conductance in a Two-Dimensional Periodic Potential, Phys. Rev. Lett. **49**, 405 (1982).

[7] F. D. M. Haldane, Model for a Quantum Hall Effect without Landau Levels: Condensed-Matter Realization of the "Parity Anomaly", Phys. Rev. Lett. **61**, 2015 (1988).

[8] C.-X. Liu, S.-C. Zhang, and X.-L. Qi, The quantum anomalous Hall effect: Theory and experiment, Annu. Rev. Condens. Matter Phys. **7**, 301 (2016).

[9] R. E. Prange and S. M. Girvin, eds., *The Quantum Hall Effect*, Graduate Texts in Contemporary Physics (Springer-Verlag, New York, 1987).

[10] S. A. Parameswaran, R. Roy, and S. L. Sondhi, Fractional quantum hall physics in topological flat bands, C. R. Phys. **14**, 816 (2013), topological insulators / Isolants topologiques.

[11] E. J. Bergholtz and Z. Liu, Topological flat band models and fractional chern insulators, Int. J. Mod. Phys. B **27**, 1330017 (2013).

[12] C.-Z. Chang, J. Zhang, X. Feng, J. Shen, Z. Zhang, M. Guo, K. Li, Y. Ou, P. Wei, L.-L. Wang, Z.-Q. Ji, Y. Feng, S. Ji, X. Chen, J. Jia, X. Dai, Z. Fang, S.-C. Zhang, K. He, Y. Wang, et al., Experimental observation of the quantum anomalous Hall effect in a magnetic topological insulator, Science **340**, 167 (2013).

[13] G. Jotzu, M. Messer, R. Desbuquois, M. Lebrat, T. Uehlinger, D. Greif, and T. Esslinger, Experimental realization of the topological Haldane model with ultracold fermions, Nature (London) **515**, 237 (2014).

[14] M. Serlin, C. L. Tschirhart, H. Polshyn, Y. Zhang, J. Zhu, K. Watanabe, T. Taniguchi, L. Balents, and A. F. Young, Intrinsic quantized anomalous Hall effect in a moiré heterostructure Science **367**, 900 (2019).

[15] M. Xie and A. H. MacDonald, Nature of the Correlated Insulator States in Twisted Bilayer Graphene, Phys. Rev. Lett. **124**, 097601 (2020).

[16] Y.-P. Lin and R. M. Nandkishore, Chiral twist on the high-T_c phase diagram in moiré heterostructures, Phys. Rev. B **100**, 085136 (2019).

[17] K. Hejazi, X. Chen, and L. Balents, Hybrid Wannier Chern bands in magic angle twisted bilayer graphene and the quantized anomalous Hall effect, Phys. Rev. Research **3**, 013242 (2021).

[18] Y. H. Kwan, G. Wagner, T. Soejima, M. P. Zaletel, S. H. Simon, S. A. Parameswaran, and N. Bultinck, Kekulé Spiral Order at All Nonzero Integer Fillings in Twisted Bilayer Graphene, Phys. Rev. X **11**, 041063 (2021).

[19] A. Abouelkomsan, Z. Liu, and E. J. Bergholtz, Particle-Hole Duality, Emergent Fermi Liquids, and Fractional Chern Insulators in Moiré Flatbands, Phys. Rev. Lett. **124**, 106803 (2020).

[20] C. Repellin and T. Senthil, Chern bands of twisted bilayer graphene: fractional chern insulators and spin phase transition, Phys. Rev. Research **2**, 023238 (2020).

[21] P. J. Ledwith, G. Tarnopolsky, E. Khalaf, and A. Vishwanath, Fractional chern insulator states in twisted bilayer graphene: An analytical approach, Phys. Rev. Research **2**, 023237 (2020).

[22] G. Chen, A. L. Sharpe, E. J. Fox, Y.-H. Zhang, S. Wang, L. Jiang, B. Lyu, H. Li, K. Watanabe, T. Taniguchi, *et al.*, Tunable correlated Chern insulator and ferromagnetism in a moiré superlattice, Nature (London) **579**, 56 (2020).

[23] Y. H. Kwan, Y. Hu, S. H. Simon, and S. A. Parameswaran, Exciton Band Topology in Spontaneous Quantum Anomalous Hall Insulators: Applications to Twisted Bilayer Graphene, Phys. Rev. Lett. **126**, 137601 (2021).

[24] F. Wu and S. Das Sarma, Collective Excitations of Quantum Anomalous Hall Ferromagnets in Twisted Bilayer Graphene, Phys. Rev. Lett. **124**, 046403 (2020).

[25] See Supplemental Material at http://link.aps.org/supplemental/10.1103/PhysRevB.105.235121 for analysis of exciton binding, exciton projection of QH wave functions, and details of numerical studies.

[26] K. Yang, Dipolar Excitons, Spontaneous Phase Coherence, and Superfluid-Insulator Transition in Bilayer Quantum Hall Systems at $\nu = 1$, Phys. Rev. Lett. **87**, 056802 (2001).

[27] Y.-H. Zhang, Composite fermion insulator in opposite-fields quantum Hall bilayers (2018), arXiv:1810.03600 [cond-mat.str-el].

[28] M. A. Metlitski, D. F. Mross, S. Sachdev, and T. Senthil, Cooper pairing in non-Fermi liquids, Phys. Rev. B **91**, 115111 (2015).

[29] K. Moon, H. Mori, K. Yang, S. M. Girvin, A. H. MacDonald, L. Zheng, D. Yoshioka, and S.-C. Zhang, Spontaneous interlayer coherence in double-layer quantum hall systems: Charged vortices and Kosterlitz-Thouless phase transitions, Phys. Rev. B **51**, 5138 (1995).

[30] Y. B. Kim, C. Nayak, E. Demler, N. Read, and S. Das Sarma, Bilayer paired quantum Hall states and Coulomb drag, Phys. Rev. B **63**, 205315 (2001).

[31] F. D. M. Haldane, Fractional Quantization of the Hall Effect: A Hierarchy of Incompressible Quantum Fluid States, Phys. Rev. Lett. **51**, 605 (1983).

[32] X. G. Wen and A. Zee, Shift and Spin Vector: New Topological Quantum Numbers for the Hall Fluids, Phys. Rev. Lett. **69**, 953 (1992).

[33] J. Alicea, O. I. Motrunich, G. Refael, and M. P. A. Fisher, Interlayer Coherent Composite Fermi Liquid Phase in Quantum Hall Bilayers, Phys. Rev. Lett. **103**, 256403 (2009).

[34] C. L. Kane and M. P. A. Fisher, Quantized thermal transport in the fractional quantum hall effect, Phys. Rev. B **55**, 15832 (1997).

[35] B. Spivak and S. A. Kivelson, Phases intermediate between a two-dimensional electron liquid and Wigner crystal, Phys. Rev. B **70**, 155114 (2004).

[36] M. M. Fogler, Stripe and bubble phases in quantum Hall systems, in *High Magnetic Fields: Applications in Condensed Matter Physics and Spectroscopy*, edited by C. Berthier, L. P. Lévy, and G. Martinez (Springer, Berlin, 2001), pp. 98–138.

[37] N. R. Cooper, E. H. Rezayi, and S. H. Simon, Vortex Lattices in Rotating Atomic Bose Gases with Dipolar Interactions, Phys. Rev. Lett. **95**, 200402 (2005).

[38] N. Cooper, Rapidly rotating atomic gases, Adv. Phys. **57**, 539 (2008).

[39] Y. H. Kwan, S. A. Parameswaran, and S. L. Sondhi, Twisted bilayer graphene in a parallel magnetic field, Phys. Rev. B **101**, 205116 (2020).

[40] P. Ghaemi, J. Cayssol, D. N. Sheng, and A. Vishwanath, Fractional Topological Phases and Broken Time-Reversal Symmetry in Strained Graphene, Phys. Rev. Lett. **108**, 266801 (2012).

[41] Y. Hu, J. W. F. Venderbos, and C. L. Kane, Fractional Excitonic Insulator, Phys. Rev. Lett. **121**, 126601 (2018).

[42] N. Stefanidis and I. Sodemann, Excitonic laughlin states in ideal topological insulator flat bands and possible presence in moiré superlattice materials, Phys. Rev. B **102**, 035158 (2020).